Supplemental Material

Temperature dependence and capping and underlayer layers effect on the interfacial magnetic properties of Ir/Fe- or Pt/Fe-based systems

Djoudi Ourdani[1], N. Challab[1], Yves Roussigné[1], Salim Mourad Chérif[1], Mihai Sebastian Gabor[2,*] and Mohamed Belmeguenai [1,**]

[1] Université Sorbonne Paris Nord, *LSPM, CNRS, UPR 3407, F-93430 Villetaneuse, France*

[2] *Center for Superconductivity, Spintronics and Surface Science, Physics and Chemistry Departament, Technical University of Cluj-Napoca, Str. Memorandumului No. 28 RO-400114 Cluj-Napoca, ROMANIA*

S1. Sample structure

S2. Ferromagnetic resonance measurements

S3. Brillouin light scattering measurements

S4. Temperature-dependent measurements

S1. Samples structure

Several systems involving a Pt/Fe or Ir/Fe interface with variable Fe thickness have been grown by sputtering using various capping or buffer layers (see figure S1). TThe order of Ir in the stack has been changed to check the sign of the Ir-induced iDMI and obtained results will be compared to that of Pt. Finally, to check the obtained iDMI sign of Ir we combined Ir and Pt in the same stack to have additive or cancelling total iDMI, depeinding on the the Ir-induced iDMI sign. For comparison, symmetrical structures incorporating Cu buffer and capping layers were also grown in the same conditions.

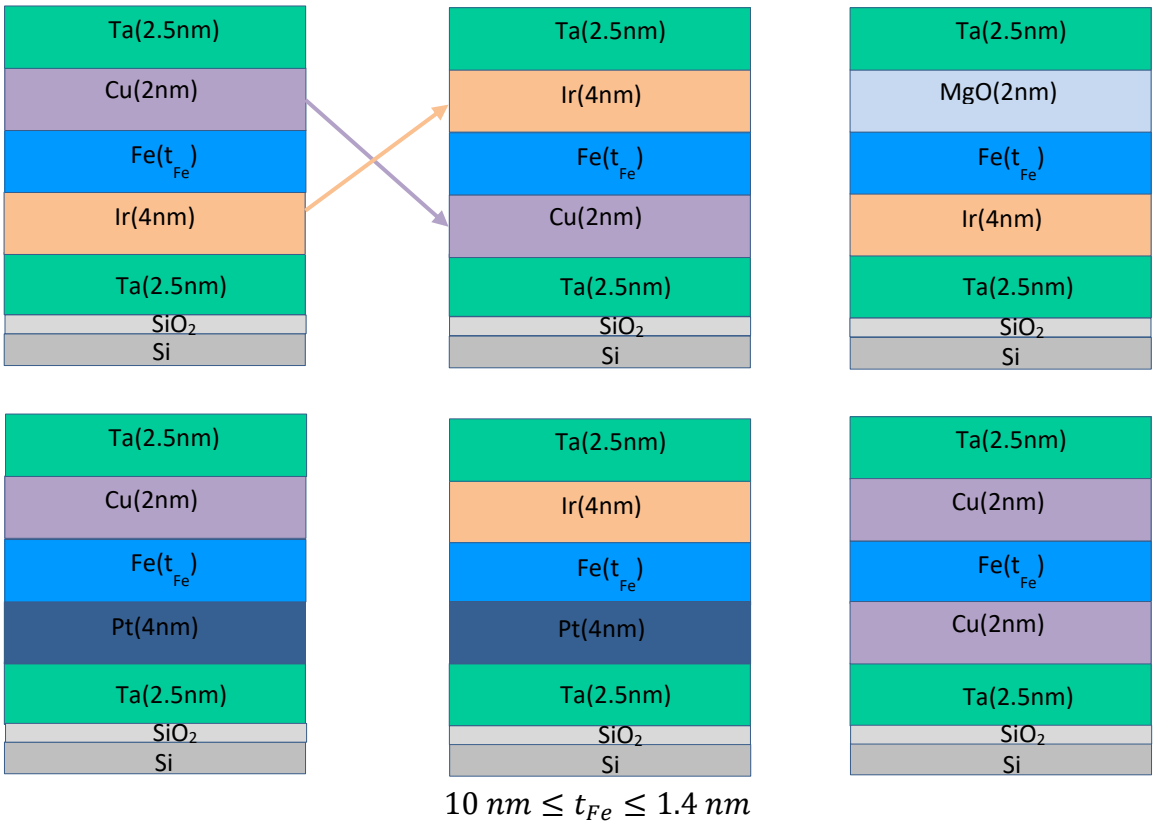

Figure S1: Stack of the various Ir- and Pt-based systems with the symmetrical Cu/Fe/Cu system with a variable fe thickness.

S2. Ferromagnetic resonance measurements

Sweep-field microstrip ferromagnetic resonance (MS-FMR), where the external applied magnetic field (up to 1.5 T) is modulated at 170 Hz by small (4 Oe) alternating magnetic field, was used to investigate perpendicular magnetic anisotropy and damping. The recorded spectra for each driving microwave frequency (shown in figure S2-1) were fitted by spectra using equation (1), to obtain the resonance field (H_R) and the and the half linewidth at half maximum (ΔH) FMR linewidth, as shown in figure S1a.

$$\frac{dP_{ab}}{dH} = A_0 \frac{-2\Delta H(H-H_R)\cos(\delta)+[\Delta H^2-(H-H_R)^2]\sin(\delta)}{[\Delta H^2-(H-H_R)^2]^2} + A_1 \quad (1)$$

Where P_{ab} is the absorbed power, δ denotes the mixing angle between dispersive and dissipative components, A_0 is the amplitude and A_1 is an offset value.

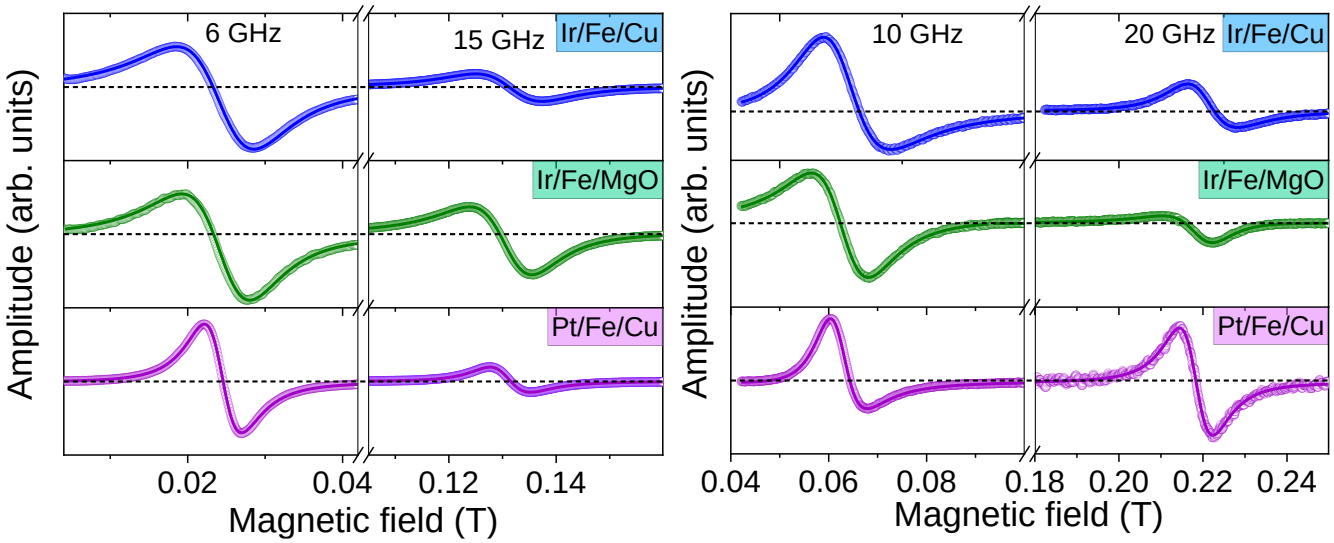

Figure S2-1: Ferromagnetic resonance spectra (measured at different driven frequencies and magnetic and applied magnetic field along the substrate edges) representing the amplitude of the field derivative of the absorbed power as a function of the in plane applied magnetic field for the 10 nm thick Fe film in 3 different systems. Symbols refer to experimental data and solid lines are linear fits using equation (1).

The microwave driving frequency versus the perpendicular to the film plane resonance field, shown in figure S2-2a, is used to determine the gyromagnetic ratio ($\gamma/2\pi$=g×13.97 GHz/T, where g is the Landé factor), while its variation as a function of the in-plane applied magnetic field, shown figure S2-2b, allowed to obtain the effective magnetization (defined as $\mu_0 M_{eff} = \mu_0 M_s - \frac{2K_\perp}{M_s}$, where $K_\perp$ is the PMA constant), using equations (2) and (3), respectively. High magnetic resonance fields beyond 1.5 T are needed, especially for the thicker films (t_{Fe}≥2 nm) of all most the studied systems, to saturate the magnetization and thus to have experimental data over a large enough frequency range to precisely determine the g-factor. Therefore, the measurement of the gyromagnetic factor was restricted to a limited range of the Fe thickness and systems as shown in figure S2-3a. The obtained value for these systems ($\gamma/2\pi$=29.8±0.5) was used for all the Fe thicknesses of the various systems. We should mention that this gyromagnetic ratio dose not vary significantly with the Fe thickness as we reported in previous

work [1] on FeV where its variation with FeV thickness was estimated of about 6% over the whole FeV investigated thickness.

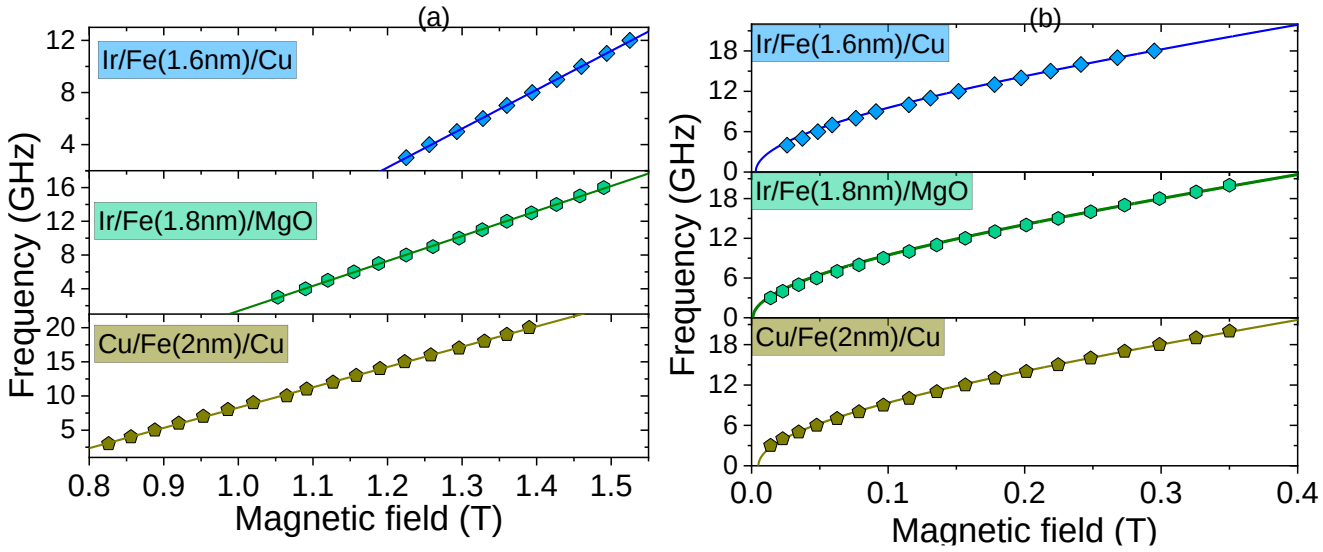

Figure S2-2: Variations of the microwave driving frequency versus (a) the perpendicular to the film plane and (b) the in-plane applied magnetic fields for various systems. Symbols refer to experimental data and solid lines are fits using equations (2) and (3).

$$F_{\perp} = \mu_0 \frac{\gamma}{2\pi}\left(H_{\perp} - M_{eff}\right) \quad (2)$$

$$F_{//} = \mu_0 \frac{\gamma}{2\pi}\sqrt{H_{//}\left(H_{//} + M_{eff}\right)} \quad (3)$$

The frequency dependences of ΔH are shown in figures S2-3a and S2-3b for all samples with t_{Fe}=10 nm and 2.8 nm respectively. Note the significantly different behavior of ΔH for the samples with the thicker Fe layers. Indeed, for t_{Fe}=10 nm and in the low frequency regime, ΔH increases rapidly with increasing driving microwave frequency. The slope of ΔH versus the frequency is system-dependent. It changes around 11 GHz. It then becomes negative for Pt/Fe/Cu, Pt/Fe/Ir, Ir/Fe/Cu and Ir/Fe/MgO systems in the frequency range of 11-18 GHz before starting to increase again above 18 GHz. The Precise determination of the Gilbert damping constant (α) needs measurements of ΔH for higher frequencies but unfortunately our MS-FMR setup does not allow measurements beyond 20 GHz. Note the "knee" behavior of the frequency dependence of the FMR linewidths for the above-mentioned systems, which is less pronounced for Cu/Fe/Cu and Cu/Fe/Ir. This dependence becomes almost linear

for the 10 nm thick Cu/Fe/Cu. For the thinner Fe, ΔH versus the frequency becomes more linear for all systems, as shown in figure S2-3b for t_{Fe}=2.8 nm. Such nonlinear behavior of ΔH versus the frequency is considered to be due to the two magnon scattering by the defects or dislocations [2, 3] since ΔH of thin films without any imperfections is expected to be proportional to the driving frequency due to the Gilbert damping. Thus, the "knee" behavior is a characteristic of a frequency dependence of ΔH dominated by the two magnon scattering mechanism. This is consistent with the strong low frequency slope of ΔH for the samples showing "knee" behavior, as presented in figure S2-3a. Note also the lower slope of the frequency dependence of ΔH in perpendicular applied magnetic field shown in figure S2-3C, where two magnon scattering contribution vanishes, confirming an extrinsic two magnon scattering contribution for the in-plane frequency dependence of ΔH. These perpendicular-field linewidth measurements were only possible for some Fe thicknesses and for a few systems, due to the low signal-to-noise ratio in this configuration and the weak magnetic field available on our MS-FMR set up. It will be discussed below. Indeed, for the thicker Fe films ($t_{Fe}\geq 2$ nm) and for the various systems, high magnetic resonance fields beyond 1.5 T (the maximum applied magnetic field available in our MS-FMR set-up) are needed to saturate the magnetization perpendicularly to the film plane and thus measure the frequency dependence of the ΔH over a large enough frequency range to precisely determine the Gilbert damping. Therefore, the measurements of the Gilbert damping was not possible for all thicknesses and for the different systems. Furthermore, as the thickness decreases, damping increases due to the spin pumping and the "knee" in the frequency dependence of ΔH becomes less pronounced and even linear. It is worth to note that the nonlinearity of the two magnon scattering is weak, and according to [22], for $F << \mu_0 \gamma M_{eff}$, the two magnon contribution is to a good approximation linear in frequency. This lack of nonlinearity in the frequency dependence of the in-plane ΔH of the thinner Fe films combined with the impossibility of measuring ΔH with a perpendicular applied magnetic fields prevent fitting of the experimental data, including all three contributions (inhomogeneity, Gilbert and two magnon scattering)

to ΔH, because the fitting parameters in this case are highly correlated and not unique. Therefore, for these samples showing a linear behavior of ΔH (see figure 3b), linear fit is used to deduce the effective value of α (α_{eff}).

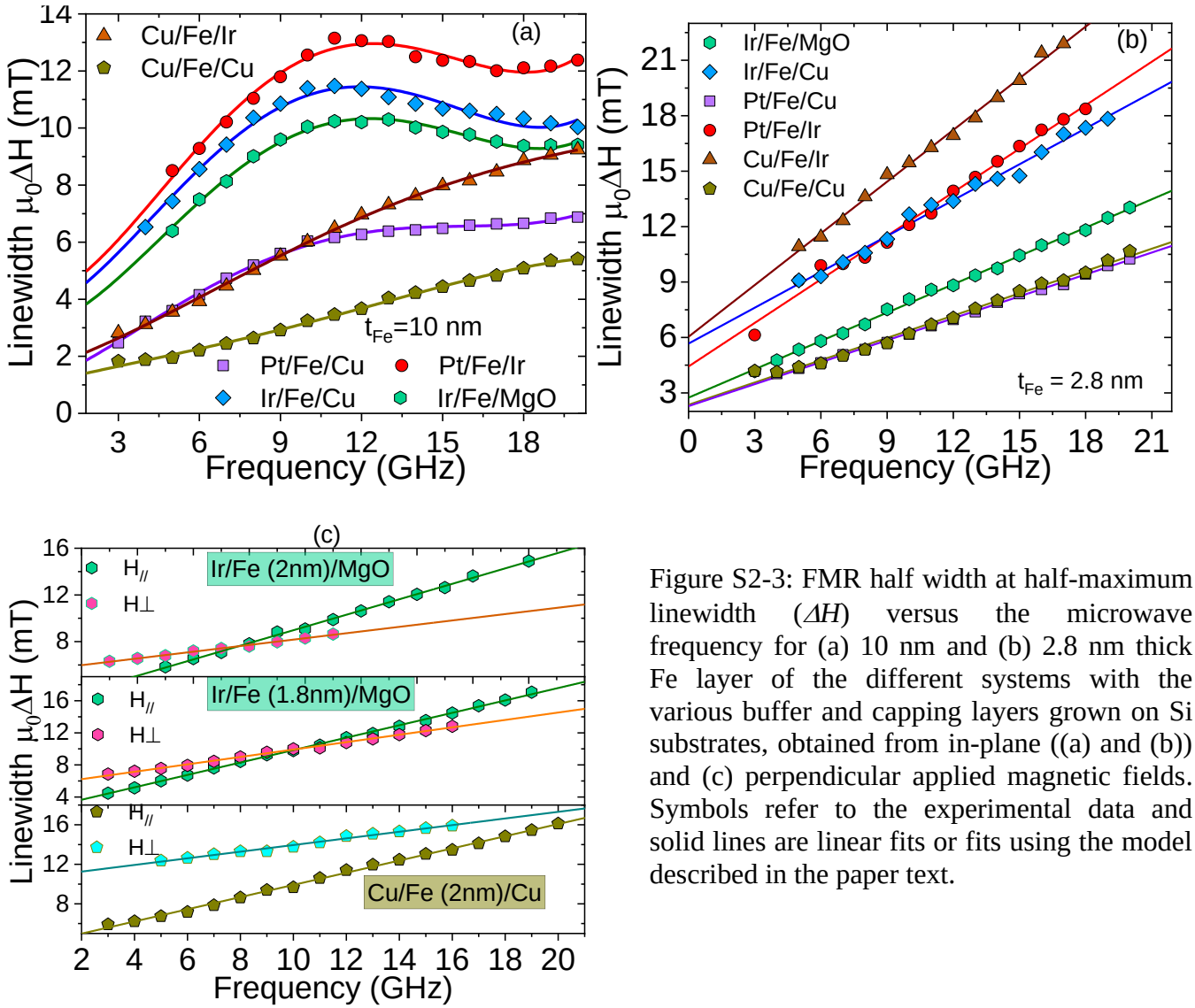

Figure S2-3: FMR half width at half-maximum linewidth (ΔH) versus the microwave frequency for (a) 10 nm and (b) 2.8 nm thick Fe layer of the different systems with the various buffer and capping layers grown on Si substrates, obtained from in-plane ((a) and (b)) and (c) perpendicular applied magnetic fields. Symbols refer to the experimental data and solid lines are linear fits or fits using the model described in the paper text.

To confirm the two magnon scattering contribution (without discussing its correlation with the microstructure), the frequency dependences of ΔH characterized by a nonlinear behavior have been fitted using the relation $\mu_0\Delta H = \mu_0\Delta H_0 + \frac{2\pi}{\gamma}\alpha F + \mu_0\Delta H_{TM}$, where $\mu_0\Delta H_{TM} = a\left|\frac{dF(H)}{dH}\right| D_{TM}(F)$ [4], to determine the magnetic Gilbert damping (α), the inhomogeneous (ΔH_0) and the two magnon scattering contributions for all systems. Here, a is the two magnon scattering amplitude, $D_{TM}(F)$ is the density of

state for the low-energy spin wave, which can be calculated numerically from the dispersion relation for the low-energy spin wave [4-6]. $F(H)$ is the field dependence of the uniform precession frequency [1]. A detailed discussion for the different microstructural contributions to $D_{TM}(F)$, which is out of the scope of this paper, has been reported by Wu et al. [7].

The nonlinear frequency dependences of ΔH have been fitted with the above equation with varying a and α as a fitting parameters. The other parameters of the fit were determined from the data of MS-FMR measurements of field dependence of the frequency. The exchange stiffness constant, involved in $D_{TM}(F)$, was assumed to be 20 pJ/m. The fits, with solid curves, are superimposed to the experimental data in figure S2-3a where a good agreement is obtained using the proper parameters.

Besides the magnetization relaxation, the FMR linewidth gives information about and samples inhomogeneities. Note the significantly higher ΔH_0 for perpendicular to the plane applied magnetic field ($\Delta H_{0\perp}$) compared to that when the magnetic field is applied in the film plane ($\Delta H_{0//}$) as revealed in figure S2-3c. Indeed, ΔH_0 is associated with an extrinsic contribution to the linewidth and reflects effects of the magnetic and structural inhomogeneities in the layers and of the two magnon scatterings. In-plane and perpendicular FMR measurements of ΔH allow one to separate inhomogeneity and two magnon scattering contributions, since for inhomogeneities, a line broadening in the perpendicular configuration ($\Delta H_{\perp}$) is expected compared to the parallel configuration ($\Delta H_{//}$). It is worth mentioning the higher $\Delta H_{\perp}$ values for Cu/Fe/Cu over the whole investigated frequency range compared to $\Delta H_{//}$ suggesting more inhomogeneous interface anisotropy. Therefore, following Mo et al. [8], we assume that "there are two dominant linewidth contributions: inhomogeneity line broadening and two magnon grain boundary scattering". The contribution due to inhomogeneity is large with a perpendicular applied field and can be negligible for an in-plane field as shown below with a simple calculation. At variance, the two magnon contribution is zero in the perpendicular geometry and large for in-plane applied field. This difference explains our experimental data shown in figure S2-3c: a large up shift of the linewidth is observed in the perpendicular configuration due to inhomogeneity $\Delta H_{\perp inhom} = 2(\Delta K)/(\mu_0 M_s)$, where ΔK is the magnitude of anisotropy variation; a noticeable increase of the slope of the linewidth variation is observed for in-plane field ; it is due to two magnon scattering.

For perpendicular applied magnetic field:

$F_{\perp} = \mu_0 \frac{\gamma}{2\pi}\left(H_{\perp} - M_{eff}\right)$ thus $\mu_0 H_{\perp} = \frac{2K_{\perp}}{M_s} - \mu_0 M_s + \frac{2\pi F_{\perp}}{\gamma}$ and $\frac{\partial H_{\perp}}{\partial K_{\perp}} = \frac{2}{\mu_0 M_s}$

For in- plane applied magnetic field: $F_{//} = \mu_0 \frac{\gamma}{2\pi}\sqrt{H_{//}\left(H_{//} + M_{eff}\right)}$

thus $\mu_0 H_{//} = \frac{K_\perp}{M_s} - \frac{\mu_0 M_s}{2} - \sqrt{\left(\frac{K_\perp}{M_s} - \frac{\mu_0 M_s}{2}\right)^2 + \left(\frac{2\pi F_{//}}{\gamma}\right)^2})$

and $\frac{\partial H_{//}}{\partial K_\perp} = \frac{1}{\mu_0 M_s}\left(1 - \left(\frac{\mu_0 M_s}{2} - \frac{K_\perp}{M_s}\right) \Big/ \sqrt{\left(\frac{K_\perp}{M_s} - \frac{\mu_0 M_s}{2}\right)^2 + \left(\frac{2\pi F_{//}}{\gamma}\right)^2}\right) < \frac{1}{\mu_0 M_s}$

Therefore, $\frac{\partial H_{//}}{\partial K_\perp} < \frac{\partial H_\perp}{\partial K_\perp}$:the contribution due to inhomogeneity is at least two times lower for in-plane applied magnetic field. This could explain the higher $\Delta H_{0\perp}$ compared to $\Delta H_{0//}$.

S3. Brillouin light scattering measurements

iDMI manifests itself by introducing a non-reciprocity of spin wave propagation, where that two spin waves with the same wave vector propagating in opposite directions do not have the same frequency. Therefore, the BLS was used to study this effect in the various systems using Pt/Fe and Ir/Fe. The sample is placed in the air gap of an electromagnet generating an in-plane magnetic field that can be varied up to 13 kOe. Monochromatic green laser (with a wavelength of λ = 532 nm) beam with a long coherence length is split into two parts by a beam splitter: a reference beam, used in the Fabry-Pérot tandem settings, and the second part, used as a probe, is focused on the sample after passing through a set of mirrors and lenses. The laser beam backscattered by the sample (elastic and inelastic processes) is directed towards a Fabry-Perot tandem to determine the frequency shift with respect to the reference (Stokes and anti-Stokes frequencies) after passing through an analyzer to reduce and eliminate the signal associated with the presence of phonons. The wave vector (k_{sw}) is determined by the angle of incidence of the laser (θ_{inc}) using the relation $k_{sw} = \frac{4\pi \sin(\theta_{inc})}{\lambda}$.

The aim is to measure the intensity and sign of iDMI, particularly for Ir, which still seems to be the subject of debate. For this, BLS spectra were acquired for different spin wave vector (k_{sw}) values and under the application of a magnetic field strong enough to saturate the in-plane magnetization (Damon-Eshbach configuration). These spectra were then fitted with a Lorentzian to determine the Stokes (S) and anti-Stokes (aS) frequencies and their frequency difference ($\Delta F = F_S - F_{aS}$) to investigate its variations of the versus the spin wave vector (k_{SW}) to measure the iDMI strength. Due to the weak iDMI values induced by Ir/Fe interface, we limited the determination of the iDMI effective constant (D_{eff}) for some systems to the measurement of ΔF at maximal k_{sw} =20.45 μm^{-1} (corresponding to incidence angle of 60°) without crossed analyser. The probed bulk phonon S and aS lines, present in the measured BLS spectra besides those corresponding to magnons, were used to check the zero frequency setting and to

proceed to frequency correction (in case of incorrect adjustment of the zero frequency) for a precise measurement of the iDMI constant [9].

The typical BLS spectra, shown in figure S3a for the various systems, revealed a frequency mismatch between Stokes and anti-Stokes with a system-dependent sign and strength. This non-reciprocity could be attributed to asymmetry of the magnetic film properties due to an interface perpendicular magnetic anisotropy [10] and iDMI contribution. However, iDMI contribution varies linearly as $1/t_{eff}$ while non-reciprocity due to the interface anisotropy difference scales linearly with the wave vector and quadratically with the t_{eff} thickness for thicknesses of 20 nm and below. Therefore, ΔF. of the thinner Fe films (below 5 nm) has been used to determine D_{eff} from the relation $\Delta F = D_{eff}\frac{4\gamma}{2\pi M_s}k_{sw} = D_s\frac{4\gamma}{2\pi M_s t_{eff}}k_{sw}$, where $D_{eff}=D_s/t_{eff}$ and D_s is the iDMI surface constant, characterizing the iDMI strength. For this and for system with significant iDMI such Pt/Fe/Cu, the linear fit of the k_{sw}-dependence of ΔF (shown in figure S3b) is used while for system showing a weak iDMI D_{eff}, is directly determined from the measured value of ΔF for k_{sw} =20.45 µm^{-1}.

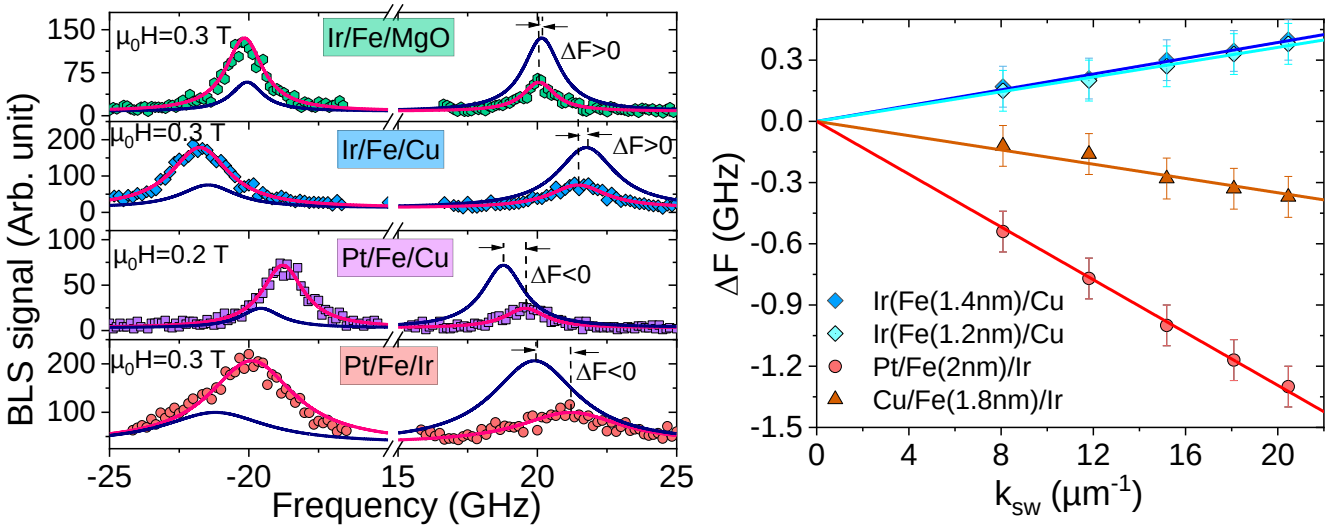

Figure S3: (a) BLS spectra measured for different Fe-based systems with various capping and buffer layers measured, at different in-plane applied magnetic field values and at a spin wave vector k_{sw} = 20.45 µm^{-1}. Symbols refer to experimental data and solid lines are the Lorentzian fits. Fits corresponding to negative applied fields (navy lines) are presented for clarity and direct comparison of the Stokes and anti-Stokes frequencies. (b) Wave vector (k_{sw})-dependence of the experimental frequency mismatch ΔF of different Fe-based systems. Symbols are experimental data and solid lines refer to linear fit.

S4. **Temperature-dependent measurements**

The temperature-dependent measurements were carried out with BLS to investigate the effect of the measurement temperature (operating temperature) on the PMA and iDMI. For this purpose, we have developed an *in situ* homemade system that we integrated into the BLS setup (see figure S4-1). This system, inserted in the electromagnet gap of the BLS setup, consists of a small cylindrical oven with an internal diameter of 1 cm and an electrical resistance of 380 Ω, connected to a direct current source. The sample is inserted inside the oven and the inside temperature is measured in real time via a probe. This temperature was varied from ambient to 250°C. For each temperature, heating, thermal equilibrium and spectrum acquisition take approximately two hours. The iDMI and the anisotropy constants are then determined from the thickness dependences of the effective magnetization and effective iDMI constant according to the method explained above.

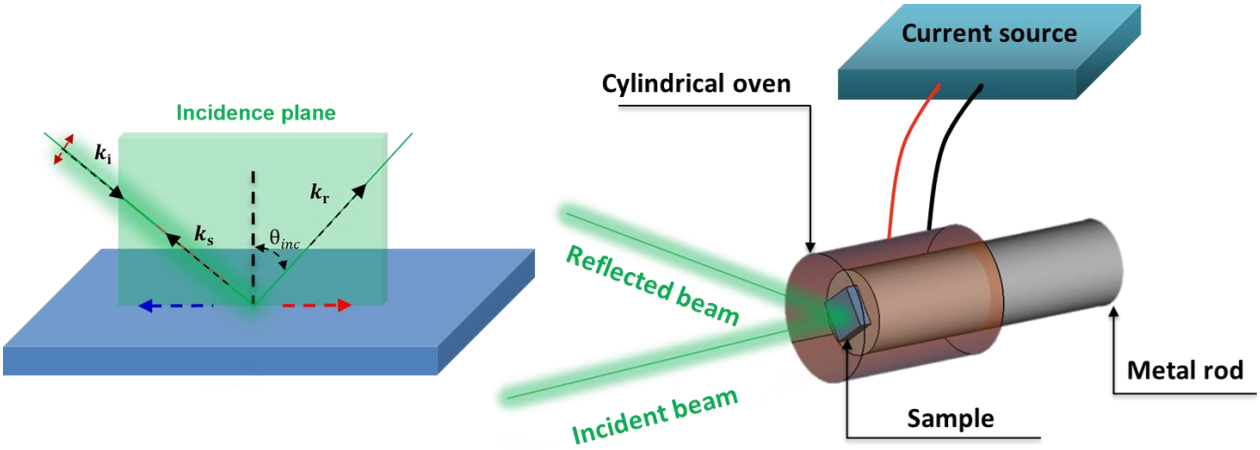

Figure S4:-1: Experimental set up showing the system used for temperature measurements: it consists of a cylindrical oven into which the sample is inserted. The oven-sample assembly is placed in the air gap of the electromagnet of the BLS set up. The temperature is varied in the range RT-250°C by applying DC current up to 250 mA. The left panel refers to schematic depicting orientations of the incident (k_i), reflected (k_r) and backscattered (k_s)wave vectors as well as the Stokes and anti-Stokes magnons.

The variations of mean Stokes and anti-Skoes line widths, measured at a magnetic field of 0.2 T, as a function of temperature are shown in Figure S4-1a, where a monotonic increase is observed for both systems. Note its strong variation in the case of Cu/Fe/Cu. These variations are irreversible, as the width measured post-heating remains almost the same as that obtained at 250°C, suggesting a structural

evolution during heating, resulting from interdiffusion. The latter occur mainly at the bottom interface, confirming the weak variation of K_s of Pt/Fe/Cu with temperature.

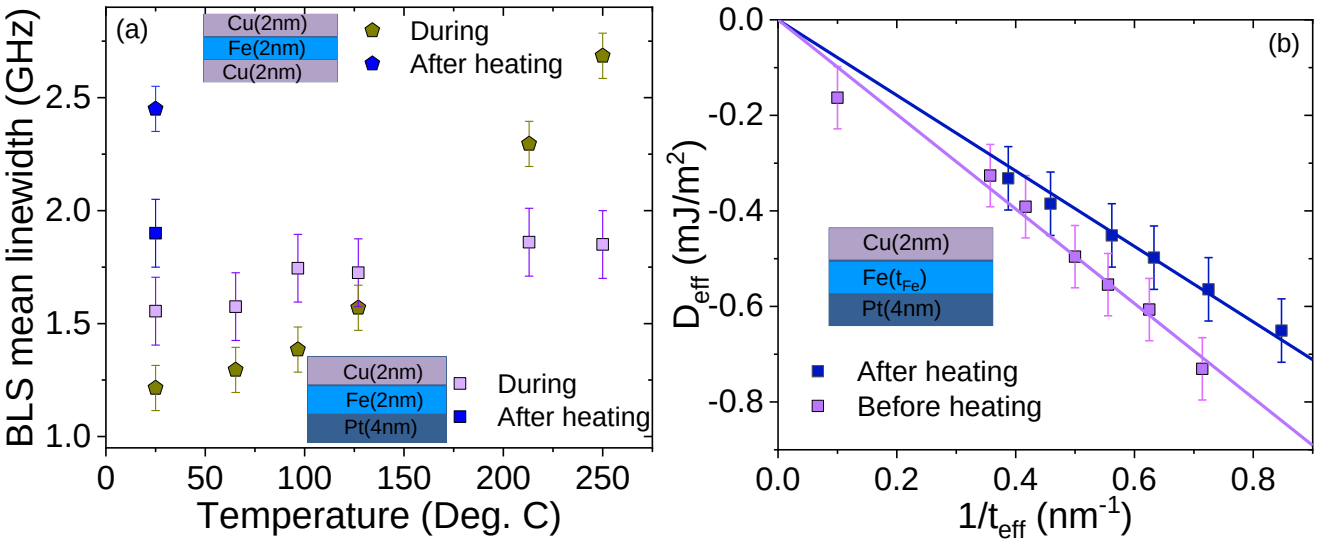

Figure S4:-2: (a) temperature dependences of the mean Stokes and anti-Skoes linewidths, measured at a magnetic field of 0.2 T for Pt/Fe(2nm)/Cu and Cu/Fe(2nm)/Cu. Blue symbols refer to values obtained after a complete temperature measurements process (RT-250°C).

References

[1] D. Ourdani, Y. Roussigné, S. M. Chérif, M. S. Gabor, and M. Belmeguenai el al. Phys. Rev. Materials 7, 034408 (2023).

[2] W. K. Peria, T. A. Peterson, A. P. McFadden, T. Qu, C. Liu, C. J. Palmstrøm, and P. A. Crowell, 'Interplay of large two-magnon ferromagnetic resonance linewidths and low Gilbert damping in Heusler thin films', Phys. Rev. B 101, 134430 (2020).

[3] R. D. McMichael, D. J. Twisselmann, and A. Kunz, Phys. Rev. Lett. 90, 227601 (2003).

[4] S. Mizukami, D. Watanabe, M. Oogane, Y. Ando, Y. Miura, M. Shirai, and T. Miyazaki, J. Appl. Phys. 105, 07D306 (2009).

[5] P. Krivosik, N. Mo, S. Kalarickal, and C. E. Patton, J. Appl. Phys. 101, 083901 (2007).

[6] R. D. McMichael, M. D. Stiles, P. J. Chen, and W. F. Egelhoff, Jr., J. Appl. Phys. 83, 7037 (1998).

[7] S. Wu, D. A. Smith, P. Nakarmi, A. Rai, M. Clavel, M. K. Hudait, J. Zhao, F. M. Michel, C. Mewes, T. Mewes, and S. Emori, Phys. Rev. B 105, 174408 (2022).

[8] N. Mo, J. Hohlfeld, M. ul Islam, C. S. Brown, E. Girt, P. Krivosik, W. Tong, A. Rebei, and C. E. Patton, 'Origins of the damping in perpendicular media: Three component ferromagnetic resonance linewidth in Co–Cr–Pt alloy films', Appl. Phys. Lett. 92, 022506 (2008).

[9] D. Ourdani, Y. Roussigné, S. M. Chérif, M. S. Gabor, and M. Belmeguenai, J. Phys. D: Appl. Phys. 55, 485004 (2022)

[10] O. Gladii, M. Haidar, Y. Henry, M. Kostylev, M. Bailleul, Phys. Rev. B, 93, 054430 (2016).